Stefanie E. STANZL-TSCHEGG*, Robert J.A. EHART**,
Elmar K. TSCHEGG**

Crack Face Interaction and Mixed Mode Fracture of Wood and Wood Composites during Mode III Loading

*Institute of Meteorology and Physics, University of Agricultural Sciences of Vienna
Türkenschanzstraße 18, A 1180 Vienna, Austria
** Institute of Applied and Technical Physics, Technical University of Vienna,
Karlsplatz 13, A 1040 Vienna, Austria

Keywords: mode I, mode III, mixed mode, fracture surface interference, wood fracture, fracture energy, wood composites

ABSTRACT: *Mode I, mode III and mixed mode fracture properties of wood and medium density fiberboard (MDF) are reported in this study. Testing procedure and specimen geometry are appropriate to obtain stable crack propagation. Thus, load displacement curves can be recorded until the specimen is completely fractured. In addition, the used testing procedure is sensitive enough to investigate the mode I crack opening induced by fracture surface asperities during mode III, which leads to mixed mode loading conditions at the crack tip. In order to better understand mixed mode fracture tests, this study concentrates on a comparison of crack propagation under pure external mode I and mode III loading conditions and on the investigation of the amount of intrinsic mode I contributions arising from fracture surface asperities during mode III loading.*

Notation

F_I	applied mode I load
F_{III}	applied mode III load
CMOD	crack mouth opening displacement (mode I)
CMSD	crack mouth sliding displacement (mode III)
M	torque from testing machine
φ	angle of twist
r	radius of loadpoint from torsional axis
$G_f^{(I)}$	specific mode III fracture energy
$G_f^{(III)}$	specific mode I fracture energy
B_{lig}	ligament width
H_{lig}	ligament length

Introduction

Fracture surfaces of materials are rough, either on a microscopic or a macroscopic scale or they have a tortuous profile. These surface structures induce crack face interactions during mode II or mode III loading of a cracked component, which influence the crack propagation behaviour during monotonic or cyclic loading effectively. In principle, two effects are observed during mode II or mode III loading of technical materials: (i) friction, abrasion, interlocking of fracture surface asperities and similar energy dissipative processes, which reduce the nominal stress values (which are calculated from the external applied loads) at the crack tip to lower effective values and (ii) additional mode I crack opening is induced owing to the sliding displacement acting on the fracture surface asperities in the vicinity of the crack tip. Therefore mixed mode loading conditions are generated at the crack tip. If on the other hand an external mixed mode load is applied the influence of crack face interactions is reduced with increasing mode I crack opening.

The effect of crack face interaction on the crack growth behaviour during sliding and mixed mode loading is known for a long time. The dependence of the crack growth rates during cyclic torsional loading on ΔK_{III} and on the crack length were first quantitative evidence for the influence of crack face interaction (1). It has been shown in (1) , that "shielding" of the crack tip by crack face interaction is much higher under mode III loading than during mode I crack propagation (2). This effect is very high especially in the threshold regime, at low cyclic stress intensity values (3). Overviews on the influence of crack face interactions on the fatigue crack growth behaviour in the Paris- and threshold regime are reported for metals in (4-8).

Interference of fracture surfaces plays a role also during fracturing under static loads and influences the measured load values by intrinsic components. Quantitative studies on the influence of crack face interactions have been performed on metals (9-11) and ceramic materials (12,13). It could be shown in general, that the measured fracture toughness values are increased considerably by crack face interactions, depending on precrack length, deformation capability of the material and fracture surface roughness.

Simulations and theoretical studies have accomplished additional information on the mechanisms of crack face interactions during mode II, mode III and mixed mode loading. First results in this field have been published by Gross and coworkers (14, 15). More recent studies on metallic materials (11, 16) show, that the amount of shielding effects by crack face interaction depends on the modulus of elasticity and the yield strength of the considered material. The most relevant microstructural parameter for ceramic materials (17) are the angle between sliding grains and the coefficient of friction between sliding grain boundaries. The grain size does not play an important role.

The influence of crack face interaction effects during mode II, mode III and mixed mode loading has been studied with homogeneous materials only until now. It has to be expected, however, that crack face interactions are especially effective in heterogeneous, disordered materials, like in particle or fiber reinforced or laminated materials. First mode III fracture studies on southern pine wood and wood composites (18) have shown, that large mode I crack openings are induced by the rough fracture surfaces, which originate from the different structure of earlywood and latewood. The aim of this paper therefore was to study the influence of crack face interaction on the fracture behaviour of wood composites under external mode III loading. It seemed especially interesting to measure and analyze mode I crack opening and resulting mixed mode loading being induced by crack face interactions. In addition, it was considered important to compare these fracture mechanical properties under mode III and mode I loading with those of solid wood.

The concept of the linear elastic fracture mechanics has been applied to characterize the fracture behaviour of homogeneous materials until now. Wood and wood composites, however, cannot be characterized in this way. One main reason for this is, that it is not possible to determine the crack length with sufficient accuracy. The transition between process zone in front of the crack tip and bridging zone in the wake is continuous, so that a clear identification of the crack tip (and therefore exact crack length) is not possible. It therefore seems problematic to apply fracture concepts, like linear elastic fracture mechanics, J-integral and -COD concept to these materials.

The concept of total work of fracture ("fracture energy concept" (19)) on the other hand has proved suitable for a characterization of quasi-brittle wood composites (20, 21 e.g.). It completely characterizes the material and does not depend on the crack length. The only restriction is, that the specimens must not be too small, so that the energy dissipative

zones in the vicinity of the crack tip can be fully generated and thus the "size-effect" is not yet effective. Therefore the concept is appropriate for an easier experimental determination of the fracture properties and the results may be used for FE modeling. This concept is used to characterize the fracture behaviour of mode III cracks in wood composites in this study.

Mode III fracture tests usually are performed with circumferentionally notched cylindrical specimens with the crack propagating from the outer specimen surface towards the cylinder axis (1,3-6,8,9 12,13). Besides the main advantage of using cylindrical specimen shapes, which is to obtain pure mode III loading condition, this geometry has some disadvantages. Small crack lengths can be achieved only and unstable crack propagation takes place quite often in brittle and quasi brittle materials during final fracture tests. In addition, the circular symmetry is not appropriate for experiments with orthotropic materials.

In order to obtain mode I crack opening, rather high axial tension are necessary for circumferentially notched cylindrical specimens, especially as long as the cracks are short. In soft materials asperities are usually too weak and smear off instead of inducing mode I crack opening in this type of specimen. As a consequence, such geometries are not sensitive enough to investigate the mode I opening induced by asperities, for example, in wood and wood composites. Contrary to a setup with cylindrical mode III specimens, the experimental setup (18) which is used in this investigation allows mode I openings even if only low intrinsic mode I loads, originating from rough fracture surfaces, are present. As a consequence it is possible to perform tests with pure external mode III loading with free mode I opening. Measurements to investigate role and mechanism of crack opening during mode III and mixed mode crack growth of wood and wood composites with an appropriate experimental setup are reported in the following.

Material, specimen geometry and experimental setup

Material

The tests were performed with panels of an (almost transversely isotropic) wood composite namely medium density fiberboard (MDF) and with solid wood (southern pine),

which is a highly orthotropic material with approximately similar structural and mechanical properties in two directions and different ones in the third, i.e. longitudinal direction. The particles of MDF are small enough, so that almost homogeneous behaviour may be expected. All specimens were stored in a climate chamber with at a temperature of 20°C and relative air humidity of 65% before testing in order to achieve equilibrium moisture content.

Specimen Geometry

The specimen geometry is rectangular and shown in Fig. 1. The MDF specimens were manufactured by gluing together five plates (16, 19, 19, 19, 16 mm), with the MDF plate as center plate and two particleboard plates as outer plates on each side.

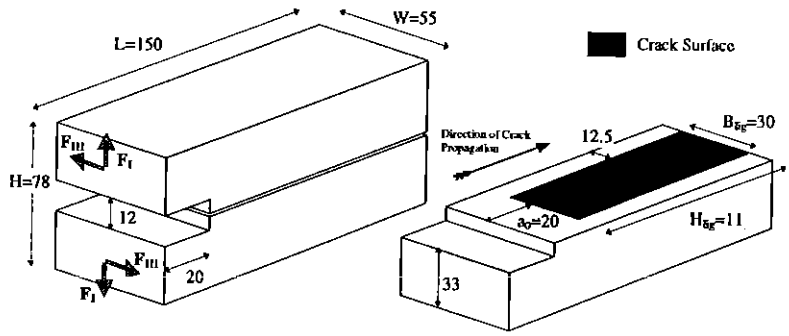

Fig. 1 Specimen geometry (dimensions in mm).

A starter notch with a depth of 20 mm and two side grooves (each 12.5 mm) were cut with a bandsaw and had a width of 1 mm. The initial notch provides the stress concentration and the side grooves help to predetermine the fracture surface. In solid wood, the grooves were cut such, that fracturing during the subsequent test took place in planes of longitudinal and radial orientation (perpendicular to year rings).

Experimental setup

The tests were performed according to the testing setup proposed by (18). A servohydraulic tension-torsion testing machine, which allows independent axial and torsional loading, both either under load or displacement control was used. Torsional axis

and direction of linear motion are parallel and oriented in vertical direction as shown in Fig. 2. Tensile loads F and resulting axial displacements from the testing machine cause mode I crack propagation, whereas torques M (torsional loads) and rotation lead to mode III loading conditions within the specimen.

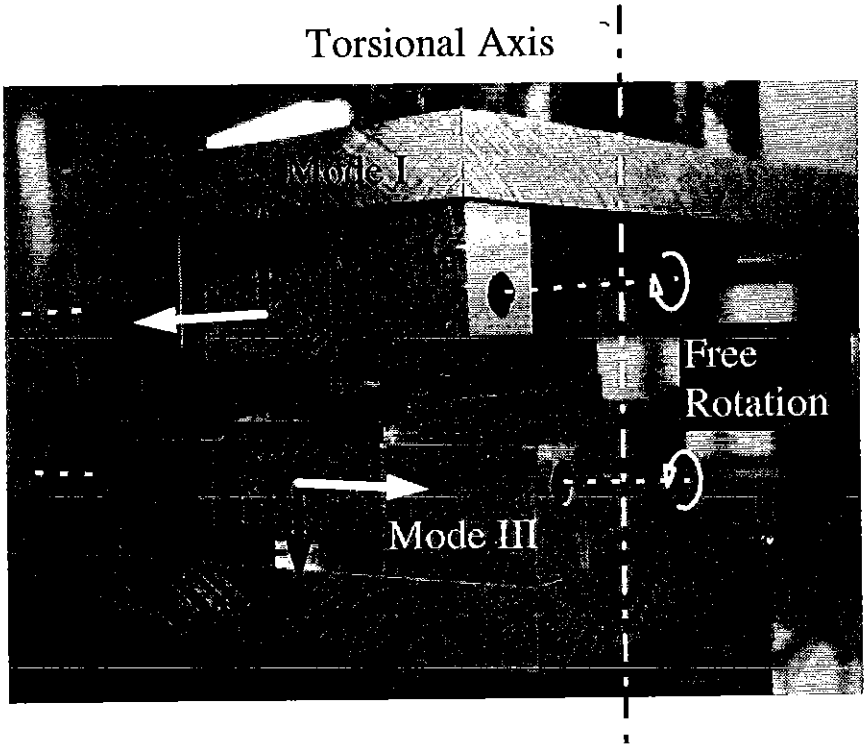

Fig. 2 Loading device with clamped specimen.

A schematic exploded view of the loading device is seen in Fig. 3. The cylinders provide the connection to the testing machine (load cell on top and actuator at the bottom) and represent the (vertical) axis of torsional twist and tensile loads (dash-dotted line in Fig. 2). The hinged loading frames are situated eccentrically on the rectangular plates and allow free rotation around an axis perpendicular to both, the torsional axis and the direction of crack propagation (white dashed lines in Fig. 2). This possibility of freedom is important to maintain the ends of the specimen free of torques associated with mode I crack openings.

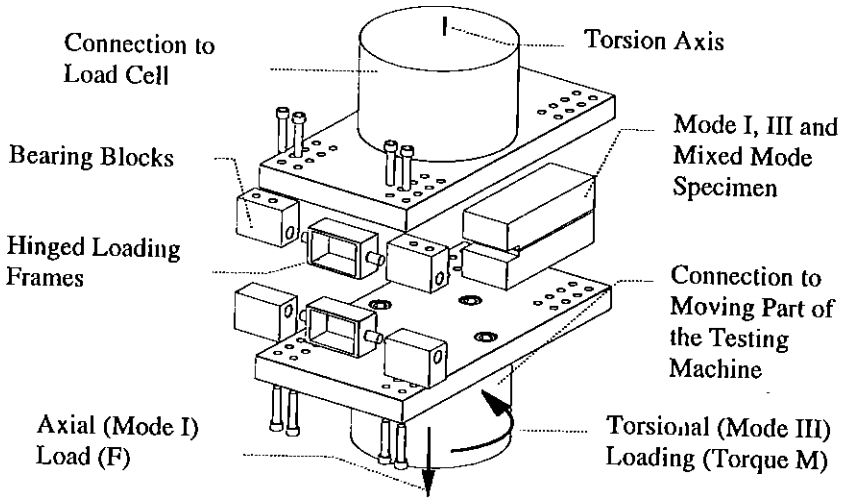

Fig. 3 Exploded view of loading device for mode I, mode III and mixed mode fracture tests.

Fig. 2 shows the assembled loading device together with a clamped specimen. The dashed lines represent the axes of free rotation of the loading frames, whereas the dash-dotted line is the torsional axis of the testing machine. Applied torque or twist around this axis results in a mode III load and displacement in the horizontal plane. Mode I load and displacement act in the vertical direction parallel to applied axial force or displacement.

Experiments and evaluation

Experimental procedure

Mode I tests were performed under displacement control preventing any torsional twist around the vertical axis (no mode III displacement). The crosshead velocity (in vertical direction) was constant with 2 mm/min.

Monotonic mode III loading was applied by a torsional movement of the testing machine under angle of twist-control, whereas mode I loading was held constant at zero. As a consequence, the mode I component, which arises from fracture surface asperities, lead to mode I crack opening. The mode III loadpoint velocity was 2 mm/min displacement. Assuming a distance of the loadpoint from the torsional axis of 160 mm, requires an angular

velocity of 0.0125 rad/min. All, twisting angle, torque, linear displacement and tensile load were recorded and stored for further evaluation.

Evaluation

Both, mode I and mode III crack propagation take place in a stable manner with the proposed setup. Therefore all data can be recorded until complete separation of the specimen is obtained.

The fracture behaviour under mode I loading is characterized by load-displacement curves, where the applied load F_I is plotted versus the loadpoint displacement (crack mouth opening displacement CMOD).

The corresponding results obtained from measurements in mode III are torque and angle of twist. In order to better compare mode I and mode III results, mode III load F_{III} and displacement (crack mouth sliding displacement CMSD) are calculated from the applied torque and twisting angle according to Eq. 1 and 2, where r is the distance of the average loadpoint to the torsional axis.

$$F_{III} = \frac{M}{r} \tag{1}$$

$$CMSD = r \cdot \varphi \tag{2}$$

Although the applied external mode I load is kept constant at zero during mode III tests, mode I crack opening is observed as a consequence of the fracture surface asperities being formed during fracture and the free mode I opening capabilities of the used experimental setup. This displacement (CMOD) is plotted versus the CMSD together with the applied mode III load F_{III} (Figs. 4 and 5), in order to qualitatively characterize the amount of mode mixture.

If the specimens are large enough („size effect") and have a sufficient ratio of width to length (21,22) the shape of the load-displacement curve is characteristic for the investigated material. Three parameters, that describe the shape of the load-displacement curve are used to characterize the fracture properties of the investigated material:

Maximum load, F_{max} and initial slope, correspond to strength and stiffness, respectively and may be used for comparison purposes, if the same specimen geometry is used in all experiments.

The energy that is consumed to completely separate the specimen is calculated by integrating the load-displacement curve. Division by the ligament area yields the specific mode I and mode III fracture energy $G_f^{(I)}$ or $G_f^{(III)}$ (Eq. 3)

$$G_f^{(III)} = \frac{1}{A_{lig}} \int M \, d\varphi = \frac{1}{B_{lig} H_{lig}} \int F_{III} \, d(CMSD) \tag{3}$$

similar to that of mode I (Eq. 4)

$$G_f^{(I)} = \frac{1}{A_{lig}} \int F_I \, d(CMOD) \tag{4}$$

Results

The measured load-displacement curves of solid wood and MDF fiberboard are plotted in Fig. 4 and Fig. 5. The solid lines represent the mode III load F_{III} versus crack mouth sliding displacement CMSD. The dotted lines show the corresponding mode I crack mouth opening displacement CMOD, which is present though the external mode I (=tensile) load is zero.

The dashed lines are load-displacement curves obtained for pure mode I loading with the same specimen geometry. In order to indicate the scatter of data several curves of identical specimens are plotted.

The mode III loads F_{III} (being calculated according to equation (1)) in the load-displacement curves are much higher for both materials than the mode I values F_I. Especially the maximum loads are by more than a factor of 2 higher. The initial slopes of the curves are similar for mode I and mode III loading, and thus the maximum load values are reached at larger displacements during mode III loading.

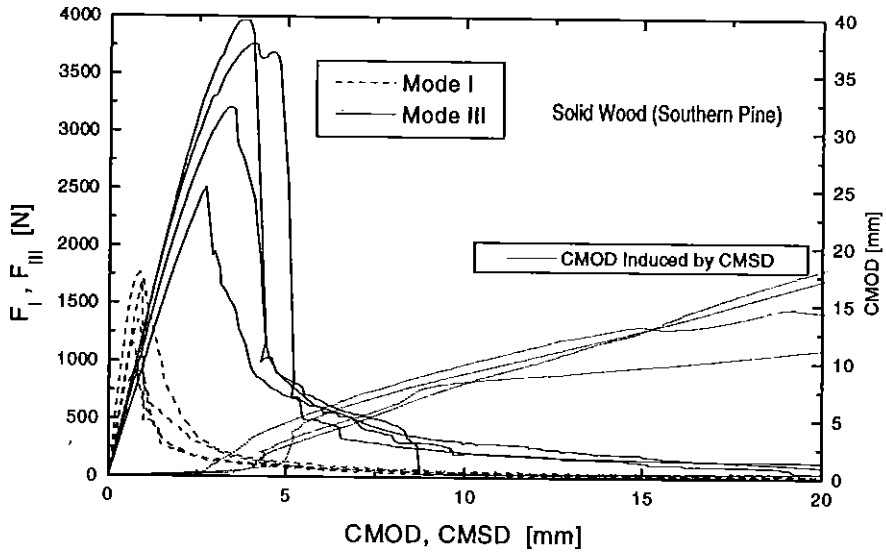

Fig. 4 Mode III load-displacement curve (solid) with superimposed axial load being zero, but intrinsic mode I opening (dotted) and mode I load-displacement curve (dashed) of solid (southern pine) wood.

The dotted lines represent the CMOD´s, which arise during mode III loading with free mode I opening. The CMOD´s increase slightly and linearly with increasing CMSD´s until the maximum mode III load value is reached in solid wood as well as in fiberboard. After this maximum load level is obtained, which is assumed to be the moment of beginning crack propagation, the CMOD´s increase steeply with increasing CMSD´s. With further increasing CMSD´s, the slope of the CMOD vs. CMSD curve decreases in fiberboard (Fig. 5) and tends towards a saturation value between approximately 1mm (in three specimens) and 2.3 mm (in one specimen). Contrary to this, the CMOD vs. CMSD curve of solid wood shows are very pronounced increase of the CMOD´s up to large CMSD values and does not reach a plateau value. Even at very large CMSD values the induced CMOD still increases.

The Mode III load-displacement curves of MDF show relatively small scatter of initial slope and shape of the decreasing part. Larger variations are observed for the maximum load. The observed values of the CMOD´s indicate, that mixed mode conditions are present at early stages of crack propagation. The initial slopes and shapes of the mode I load-displacement curves scatter more, whereas the maximum loads are closer together. Comparing mode I and mode III curves, yields similar initial slopes but a maximum load of mode III, that is by a factor 2.5 higher than that of mode I.

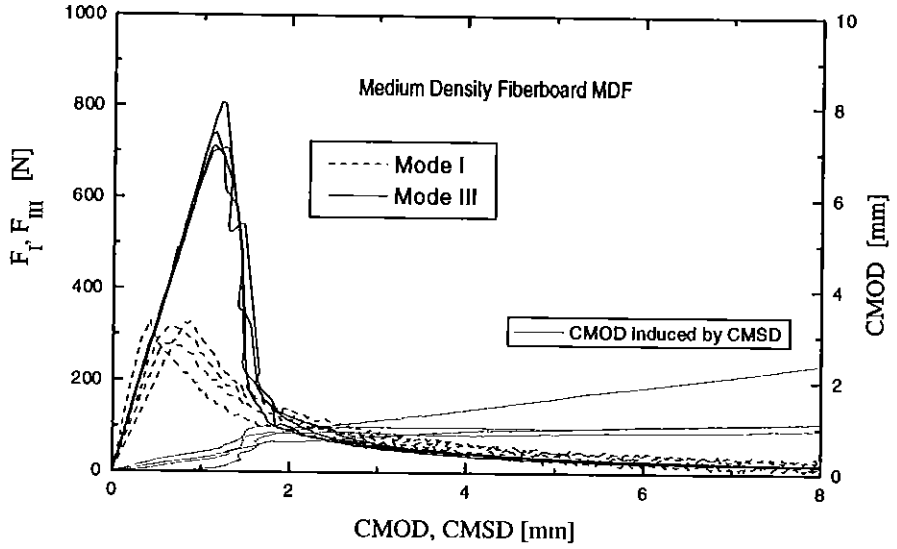

Fig. 5 Mode III load-displacement curve (solid) with superimposed axial load being zero, but intrinsic mode I opening (dotted) and mode I load-displacement curve (dashed) of medium density fiberboard (MDF).

In order to make comparison easier the characteristic parameters $G_f^{(i)}$(specific fracture energy), $F_{max}^{(i)}$ (maximum load) and initial slope of the load-displacement curves are plotted in Fig. 6, where i=I or III for mode I (left column) and mode III (right column), respectively. The G_f values of mode III are in general higher than those of mode I.

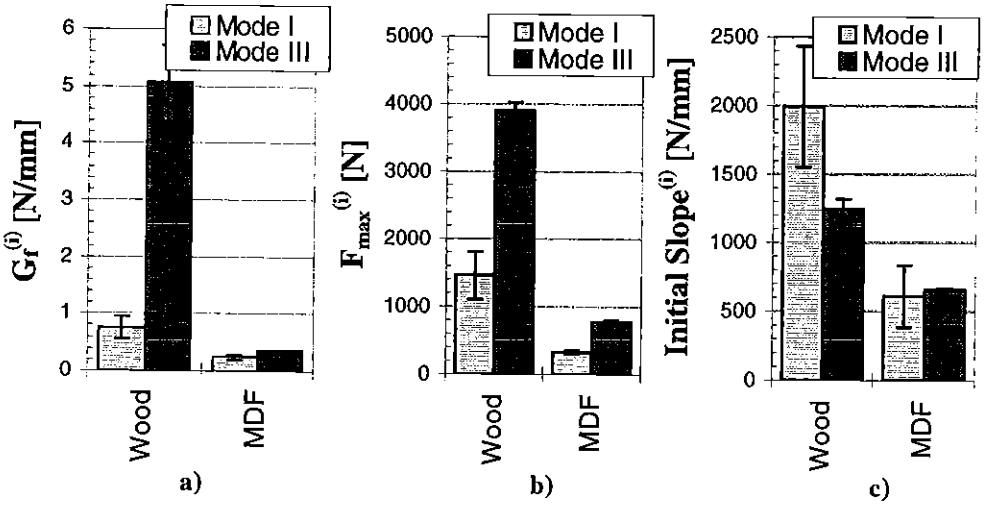

Fig. 6 Characteristic G_f, F_{max} and initial slope values of the load-displacement curves for mode I and mode III loading.

Discussion

In isotropic, brittle materials macroscopic shear fracture is often a consequence of small mode I cracks oriented perpendicular to the axis of major principal stress, which is at an angle of 45 degrees with respect to the macroscopic crack. Such behaviour was for example observed for fatigue mode III fractures of steel at low load levels by Tschegg and Stanzl (e.g. 4). Fractography of the fracture surfaces of the wood materials investigated in this study did not indicate this "factory roof" shape, but generally rough fracture surfaces.
In general, the mode I load-displacement curves are lower than the mode III curves. This is not only caused by different material behaviour under the two loadcases, but also by the fact, that sliding mode fracture is always accompanied by fracture surface interferences like friction and mutual support. This leads to crack tip shielding and consequently to a higher resistance against crack propagation.

MDF behaves almost like a homogeneous material under mode I (and also mode III) loading. The fibers are very small but to a certain degree oriented parallel to the panel plane. Fiber bridging usually takes place only at a microscopic scale. Therefore the bridging effect is not very pronounced but load-displacement curves still do not decrease steeply indicating good stability of crack propagation in both, mode I and mode III. Generally fracture is caused by debonding of the single fibers. In solid wood the fracture surfaces are microscopically smoother but large strands may be formed by crack branching, that bridge the distance between adjacent fracture surfaces. As a consequence loads either drop steeply from the maximum (if no macrofiber bridges exist) or remain at high levels otherwise, which explains the high scatter of data for solid wood.

Another, even more important effect is the intrinsic mode I component, that arises from the inclined flanks of fracture surface asperities. Shape and size of asperities determine the amount of mode mixture. It has been observed that the crack path follows grain boundaries during stress corrosion cracking in metallic materials, which results in very steep fracture surface asperities. Gross et al. (23) have shown, that in this case crack propagation under applied mode III loads actually takes place in mode I as a consequence of the induced high CMOD´s.

The different roughness of the fracture surfaces, which is caused by the different structure of solid wood and fiberboard leads to strong variations of the induced mode I opening during mode III loading. Comparing for example the maximum CMOD induced by CMSD of MDF and solid wood yields ratios of 1:15.

The fracture surface of MDF is microscopically very fibrous but this kind of roughness is made up of very weak constituents (thin fibers) and does not contribute to pronounced induced mode I opening. Macroscopically the fracture surface of MDF shows asperities of large „wavelength" (about 10 mm) but small „amplitude" (~1 mm), which corresponds to the observed induced CMOD. Contrary to this the crack front is built up of steps, that follow the interface between early and latewood in solid wood. The resulting asperities are higher and much steeper than in MDF and thus induce the much larger CMODs.

The largest differences between mode I and mode III loading arise for the specific fracture energies in solid wood. The mode III values are approximately seven times larger than the mode I fracture energies, but they are only about 20 % higher in MDF (Fig. 6a). In addition, much lower absolute values (by a factor of approximately ten) of the specific fracture energies are observed for MDF compared with solid wood.

These results show on one hand the well known superior strength of solid wood in comparison to the reconstituted wood composite MDF, where the fracture behaviour is determined by the lower strength of adhesion between fibers in comparison to cohesion within wood.

On the other hand fiber bridging plays an important role in both fracture modes (I and III) as in both materials it leads to crack tip shielding and thus increases the crack propagation resistance. Depending on the structure of the material it takes place at different scales of size: Bridging in MDF is on a microscopic scale, whereas large strands bridge adjacent fracture surfaces in solid wood. The most important influence of structure is the different amount of intrinsic mode I component. The rougher structure of fracture surfaces in solid wood leads to higher CMODs induced by mode III.

Current investigations concentrate on the influence of different kinds of particles (size and shape) on mode I crack opening induced by mode III loading.

Conclusions

1. The experimental setup allows steady state mode I and mode III crack propagation in wood and wood composites. Complete load-displacement curves can be recorded, which characterize the fracture behaviour. Several parameters like specific fracture energy can be derived from these curves.

2. The experiments can be performed in mode I, mode III and mixed mode with various testing conditions. In this work, the external mode I load was kept zero during mode III crack propagation allowing free crack opening. Fracture surface asperities transform sliding displacements into crack opening displacements. This leads to induced mixed mode conditions or even mode I dominated fracture.

3. The intrinsic CMOD can be recorded and plotted versus the CMSD together with the applied mode III load to estimate the amount of mixed mode loading condition. The testing method is sensitive enough to detect mode III induced mode I components even for wood composites with rather weak fracture surface asperities.

4. It has been detected that the induced CMOD's strongly depend on the structure of the investigated material.

5. The results of this investigation are relevant for mode II loading and also for other materials and types of composites.

References

(1) Tschegg E.K., (1982), A contribution to mode III fatigue crack propagation, Materials Science and Engineering, Vol. 54, 1982, pp. 127-137

(2) Ritchie R.O. (1979) Near-threshold fatigue crack propagation in steels, International Metals Rev. No.3 and 6, pp 205-230

(3) Tschegg E.K., (1983), The influence of a static mode I load and R ratio on mode III fatigue crack growth behaviour in mild steel, Materials Science and Engineering, 59, pp 127-137

(4) Tschegg E.K. and Stanzl S.E., (1988), The significance of sliding mode crack closure on mode II fatigue crack growth, ASTM STP 924, pp214-232

(5) Richie R.O., (1988) A comparison of fatigue crack propagation in mode I and mode III, ASTM STP 945, pp 821-842

(6) Tschegg E.K., Stanzl S.E., Mayer H.R. and Czegley M. (1992), Crack face interactions and near-threshold fatigue crack growth, Fatigue Fract. Engng Mater. Struct., Vol. 16, No. 1 pp 71-83

(7) Suresh S., (1992), Fatigue in materials, Cambridge Solid State Science Series, Cambridge University Press

(8) Tanaka K., Akinawa Y. and Nakamura H., (1996) J-Integral approach to mode III fatigue crack propagtion in steel under torsionl loading, Fatigue Fract. Engng. Mat. Struct., Vol. 5, pp 571-579

(9) Tschegg E.K. and Suresh S., (1988) Mode III fracture of 4340 steel: effects of tempering temperature and fracture surface interference, Metall. Trans. A, Vol.19A, pp 3055-3044

(10) Gross T.S., Zhang Y. and Watt D.W.,(1995) Fracture surface interference in shear - II Experimental measurements of crack tip displacement field under mode II loading in 7075-T6 Al., Acta Metall. Mater., Vol. 43, No.3, pp 901-906

(11) Gross T.S., Goulet R.U. and Mendelsohn D.A., (1996) Effect of elastic modulus and yield strength on fracture surface interference of remotely loaded mode II cracks, in press

(12) Petrovic J.J., (1985), Mixed mode fracture of hot pressed Si_3N_4, J. Am. Ceram. Soc., Vol. 68, No.6, pp 348-355

(13) Suresh S. and Tschegg E.K., Combined Mode I-Mode II Fracture of fatigue-precracked Alumina, J. Am. Ceram. Soc., Vol 70(10) pp 726-733

(14) Gross T.S., (1985) Frictional effects on mode III fatigue crack propagation, Spripta Metall., 19, pp 1185-1190

(15) Gross T.S. and Mendelsohn (1988) On the effect of crack face contact and friction due to fracture surface roughness in edge cracks subjected to external shear, Eng. Frac. Mech., 31, pp 405-420

(16) Mendelsohn D., Gross T.S., and Y. Zhang, (1995) Fracture surface interference in shear - I. A model based on experimental surface charactersistion, Acta Metall. Mater., Vol. 43, No.3, pp 893-900

(17) Hsia J.K., Zhang T.L. and Socie D. (1995), Effect of crack surface morphology on the fracture behaviour under mixed mode loading, TAM Report No. 799, UILU-ENG-95-6021, TAM Theoretical and Applied Mechanics, University of Illinois at Urbana-Champaign

(18) Ehart R.J.A., Stanzl-Tschegg S.E. and Tschegg E.K. (1996), Mode III fracture energy of wood composites in comparison to solid wood, Wood Sci. and Techn., in press

(19) Nakayama J.(1965). Direct measurement of fracture energies of brittle heterogeneous materials, J. Am. Ceram. Soc, 48 (11), 583-587

(20) Peterson H., (1992) Analysis of fracture propagation , COST 508 workshop on fracture mechanics in wooden materials, Bordeaux, France

(21) Stanzl-Tschegg S.E., Tan D.M. and Tschegg E.K., (1995) New splitting method for wood fracture characterisation, Wood Sci. and Techn. 29, pp 31-50

(22) Ehart R.J.A., Stanzl-Tschegg S.E., Tschegg E.K., (1996) Fracture Characteristics of PARALLAM® PSL in Comparison to Solid Wood and Particleboard, Wood Sci. and Techn., in press

(23) Gross T.S., Mendelsohn D.A., (1989) Mode I stress inensity factors induced by fracture surface roughness under pure mode III loading: Application to the effect of loading modes on stress corrosion crack growth, Metall. Trans. A, Vol. 20A, Oct. 1989, pp. 1989-1999

Acknowledgement :The authors gratefully acknowledge financial support of the Austrian National Bank (research project no. 4917) to purchase the tension-torsion machine.